CELL CYCLE
2023, VOL. 22, NO. 19, 2097–2112
https://doi.org/10.1080/15384101.2023.2275900

Taylor & Francis
Taylor & Francis Group

RESEARCH PAPER

Check for updates

Depleting ANTXR1 suppresses glioma growth via deactivating PI3K/AKT pathway

Chaoyang Zhou, Aijun Liang, Jianzhong Zhang, Jingxing Leng, Bin Xi, Bin Zhou, Yu Yang, Ronglan Zhu, Liangchen Zhong, Xingxing Jiang, and Dengfeng Wan

Department of Neurosurgery, Jiangxi Provincial People's Hospital the First Affiliated Hospital of Nanchang Medical College, Nanchang, Jiangxi Province, China

ABSTRACT

Gliomas are commonly known as primary brain tumors and associated with frequent recurrence and an unsatisfactory prognosis despite extensive research in the underlying molecular mechanisms. We aimed to examine the role of ANTXR1 in glioma tumorigenesis and explore its downstream regulatory mechanism. ANTXR1 expression in clinical specimens and its relationship with some pathological characteristics were detected using immunohistochemical staining. After silencing/upregulating ANTXR1 through lentiviral transfection in glioma cell lines, qRT-PCR and western blotting were used to examine mRNA and protein levels, and cell phenotype was also detected. ANTXR1-knockdown and -overexpression cells were then processed by AKT activator and PI3K inhibitor, respectively, to verify downstream PI3K/AKT pathway regulated by ANTXR1. Xenograft nude mice models were constructed to verify the role of ANTXR1 *in vivo*. We found overexpression of ANTXR1 in both cell lines in comparison with those in normal brain tissues. Glioma cell growth and migratory ability were dramatically impaired as a result of silencing *ANTXR1* by shANTXR1 lentiviruses. ANTXR1 blockade also accelerated cell apoptosis and held back cell cycle via targeting G2 phrase during cell mitosis. *In vivo* xenograft models verified *in vitro* findings above. Further exploration disclosed that AKT activator promoted anti-tumor effects mediated by ANTXR1 knockdown, while PI3K inhibitor limited pro-tumor effects mediated by ANTXR1 overexpression, indicating that ANTXR1 functioned in glioma cells through regulating PI3K/AKT pathway. ANTXR1 could play an indispensable role in glioma tumorigenesis via activating PI3K/AKT-mediated cell growth. Our study provides a theoretical basis for targeting ANTXR1 as a molecular target in glioma clinical therapeutics.

ARTICLE HISTORY
Received 30 August 2021
Revised 22 December 2022
Accepted 22 October 2023

KEYWORDS
Glioma; ANTXR1; proliferation; metastasis

1. Introduction

Brain tumors are associated with significant morbidity and mortality due to aggressiveness of local growth and metastasis within the central nervous system or to the spine [1]. Glioma was estimated to comprise 28% of brain and other central nervous system tumors, and 80% of malignant brain tumors [2], which has been considered as a primary malignant brain tumor. It is thought to originate from neuroglial stem cells and categorized as astrocytic, oligodendroglial or ependymal tumors based on the histopathologic features [3]. Typically, glioma is characterized by a high degree of infiltrative growth which contributes to frequent recurrence [4]. Despite the role of molecular markers in the determination of low-grade gliomas has been generally confirmed, i.e. *IDH1*- and *IDH2*- mutations, it is not necessarily true in the high-grade glioma, and the specific molecular markers still need further investigations [5]. To date, the therapeutic approach of glioma is usually surgical resection in conjunction with chemotherapy, radiotherapy, immunotherapy or gene therapy. However, the combined treatments were not always effective and glioma patients in many cases suffered from high risk of recurrence and a very poor prognosis [6]. Therefore, it still matters to seek for advances in therapeutic strategies of gliomas based on its molecular pathogenesis.

ANTXR1 (Anthrax toxin receptor 1), also known as Tumor endothelial marker 8 (TEM8), is encoded on chromosome 2 in human as a type I transmembrane protein and is a highly conserved cellular receptor for anthrax toxin secreted by

CONTACT Dengfeng Wan wandengfeng06@163.com Department of Neurosurgery, Jiangxi Provincial People's Hospital the First Affiliated Hospital of Nanchang Medical College, No.266, North Fenghe Road, Nanchang, Jiangxi Province, China

© 2023 Informa UK Limited, trading as Taylor & Francis Group

Bacillus anthracis [7]. The tripartite anthrax toxin is composed of protective antigen (PA), lethal factor and edema factor [8], among which the PA component binds to ANTXR1 and then the complex mediates delivery of toxin to cytoplasm. Through binding collagen types I and VI, ANTXR1 also acts a pivotal role in endothelial cell attachment and migration [9], and servers as a promoter in the process of pathological angiogenesis. ANTXR1 was originally found upregulated in the endothelial cells in angiogenesis of colorectal cancer [10] and subsequently was identified overexpressed in various cancers, such as gallbladder carcinomas, breast cancer [11] and prostate cancer [12], in comparison with that in normal tissues. A previous study suggested that the mutation in *ANTXR1* gene would lead to disorganized angiogenesis in response to the inhibitory effect on downstream signaling pathways in infantile hemangioma [13]. Besides, downregulation of ANTXR1 slowed down tumor growth in a few cancer models, including melanoma, breast cancer, colorectal cancer and lung cancer [14]. ANTXR1 acted as a downstream target of *miR-26b-3p* and its overexpression has been reported in glioma issues [15]. However, little is known about the role of ANTXR1 in the development of glioma and its downstream molecular mechanism.

In this study, we thus exploited a series of *in vitro* and *in vivo* experiments to disclose and identify biological functions of ANTXR1 in glioma progression, through which we aimed to evaluate the possibility of ANTXR1 to serve as a potential molecular therapy target. Our findings indicated the ANTXR1-mediated apoptosis via deactivating PI3K/AKT signaling pathway and underscored the vital role of ANTXR1 in glioma progression, as well as its further potential application as a targeted molecular agent.

2. Materials and methods

2.1. Clinical samples and immunohistochemical staining

Tissue microarrays of glioma samples from 134 patients (15–80 years old, glioma histopathological grade II, III and IV) and normal brain samples from 24 people were from Jiangxi Provincial People's Hospital. The usage of all samples was approved with permission from all patients and followed the International Ethical Guidelines for Biomedical Research Involving Human Subjects issued by the Council for International Organization of Medical Sciences (CIOMS). The histopathological grading of the glioma tissue microarrays here was based on the 2016 World Health Organization classification of tumors of the central nervous system [16]. In terms of immunohistochemical staining, we firstly baked the slides of glioma tissues and matched normal brain tissues in oven at 65°C for 30 min followed by dewaxing and rinsing them for several times. After retrieving the antigen by disposing with citric acid antigen at 100°C for 10 min, we blocked the slides using 3% H_2O_2 for 5 min. ANTXR1 antibody (1:250, Cat. #ab21270, Abcam) was next added to the slides at 37°C for 1 h and then the second antibody. The staining was finished after treatment of DAB and hematoxylin. Then, we photographed the slides and evaluated the staining percentage and the intensity, according to which we assigned values to each slide and determined the outcomes of immunohistochemical staining. Specifically, the assignment score of a slide was the integer from 1 to 4 when the staining percentage was less than 25%, 50%, 75% and 100%, respectively. Similarly, the staining intensity was also quantified and scored from 0 to 3 based on the color depth with 0 signifying no dyeing and 1–3 light yellow, pale brown and dark brown. Thus, the extent of antibody expression on each slide representing the expression pattern of ANTXR1 was ultimately confirmed by the assignment score multiplying staining intensity. The median of assignment scores of all sampled slides was defined as the cutoff to evaluate whether the expression pattern of ANTXR1 was high or low for each slide.

2.2. Constructing lentiviral vector

We applied human gene *ANTXR1* as the template and then designed RNA interference target sequences (5'-ATCCGTCAAGGCCTAGAAG AA-3', 5'-GACAGTAAGGATCATGTGTTT-3', 5'-CTATTCAGAGAGGGAGGCTAA-3'), while scramble sequence (5'-TTCTCCGAACGTGTCACGT-3') was used for vector construction as the negative control. Followed by the treatment of restriction endonuclease Age I and EcoR I (Cat. #R3552L and R3101L, NEB), cDNA encompassing interference sequence

was linked with the linear BR-V108 vector (Shanghai Yibeirui Biomedical science and Technology Co., Ltd.), which were then transfected into *E. coli* receptor cells (Cat. #CB104–03, TIANGEN). PCR technique was subsequently carried out to select and verify positive clones. High-purity plasmids carrying interference sequence were then extracted utilizing EndoFree midi Plasmid Kit (Cat. #DP118–2, TIANGEN). With regard to ANTXR1-overexpression cells, we cloned the cDNA sequence (upstream, 5'-AGGTGCTAAGTTGGAAAAGGC-3'; downstream, 5'-TGTTGAGATTTCGCGGCTC-3') into lentiviral vectors. In the end, we co-transfected Helper 1.0 and Helper 2.0 plasmids, as well as BR-V108 into 293T cells to successfully construct lentiviral vector.

2.3. Lentiviral transfection and qRT-PCR

Human glioma cell lines SHG-44 and U251 have been prepared, thawed from freezing and then cultured in medium (90% DMEM + 10% FBS). Cells were incubated for 24 h under 5% CO_2 at 37°C, after which transfected by shANTXR1 or shCtrl lentivirus for 72 h and photographed through fluorescence microscopy. Subsequently, the total of RNA was extracted from both cell lines and quantified using Trizol (Cat. #T9424-100 m, Sigma) and Nanodrop 2000/2000C, respectively. After reverse transcription using Hiscript QRT supermix for qPCR (+gDNA WIPER) (Cat. #R123–01, Vazyme), we obtained cDNA and then amplified by means of qRT-PCR using Hiscript QRT supermix for qPCR (+gDNA WIPER) (Cat. #R123–01, Vazyme) and AceQ qPCR SYBR Green Master Mix (Cat. #Q111–02, Vazyme). We next applied $2^{-\Delta\Delta CT}$ method to measure GAPDH as controls. The sequences of primers used were as described below:

ANTXR1, upstream sequence 5'-AGGTGCTAA GTTGGAAAAGGC-3' and downstream sequence 5'-TGTTGAGATTTCGCGGCTC-3';

GAPDH, upstream sequence 5'- TGACTTCA ACAGCGACACCCA-3' and downstream sequence 5'CACCCTGTTGCTGTAGCCAAA-3'.

2.4. Western blotting

Glioma cells were prepared and lysed by 1 × cold lysis buffer. BCA kit (Cat. #23225, HyClone-Pierce) serves to quantify proteins. After separated by 10% SDS-PAGE, protein extracts were transferred to a polyvinylidene difluoride membrane and incubated using blocking liquid for 1 h. We next probed the blots using primary antibodies of ANTXR1 (1:1000, Cat. #ab21270, Abcam), AKT (1:2000, Cat. #SAB4500796, Sigma), p-AKT (1:500, Cat. #AF887-sp, R&D), CCND1 (1:5000, Cat. #ab134175, Abcam), CDK6 (1:1000, Cat. #ab151247, Abcam), MAPK9 (1:3000, Cat. #ab76125, Abcam) and GAPDH (1:3000, Cat. #AP0063, Bioworld), and goat anti-rabbit IgG (HRP) (1:3000, Cat. #A0208, Beyotime) as secondary antibody. Moreover, when examining the influence of AKT activator or PI3K inhibitor on cell phenotype, we utilized primary antibodies AKT (1:3000, Cat. #4691S, CST), p-AKT (1:500, Cat. #9611, CST), PI3K (1:1000, Cat. #4257S, CST), p-PI3K (1:750, Cat. # bs-3332 R, Bioss), ANTXR1 (1:1000, Cat. #ab21270, Abcam) and GAPDH (1:30000, Cat. #60004–1-lg, Proteintech) with goat anti-rabbit IgG (HRP) (1:3000, Cat. #A0208, Beyotime) and goat anti-mouse IgG (HRP) (1:3000, Cat. #A0216, Beyotime) as secondary antibodies. Lastly, the signal of membranes was detected utilizing immobilon Western Chemiluminescent HRP Substrate (Cat. #RPN2232, Millipore).

2.5. Cell proliferation assay

Cell proliferation of experimental cells was examined via CCK8 assay. Cell suspension (100 μL/well) was firstly inoculated in a 96-well plate, which was then placed in an incubator for pre-culture (37°C, 5% CO_2). Before testing, the plate was added by 10 μL CCK solution (Cat. #96992, Sigma) into each well and then incubated for 1 h to 4 h. Next, the absorbance of the plate at 450 nm was measured using a microplate reader (Cat. #M2009PR, Tecan infinite). The cell growth curve was lastly plotted with time as the x-axis and the absorption value as the y-axis.

2.6. Flow cytometry (FACS)

We employed flow cytometry to examine cell apoptosis and cell cycle of both glioma cell lines. At the very beginning, the cells were trypsinized and rinsed in cold PBS (pH = 7.2 ~ 7.4). As to the detection of apoptosis, cells were then re-rinsed with 1 × binding buffer and stained by Annexin V-APC for 15 min from light. The percentage of cell apoptotic rate was thus determined by FACSCalibur (BD Biosciences). The above was flow cytometry (single staining method) to detect cell apoptosis. The following was flow cytometry (double staining method) to detect cell apoptosis. Glioma SHC-44 and U251 cells infected with shANTXR1 or shCtrl lentivirus were inoculated into 6-well plates. When the confluence reached 85%, the cells were washed once by D-Hanks. Subsequently, the cells were washed once by 1 × binding buffer, and then stained with Annexin V-APC (Cat. #10010–09, southern biotech) for 15 min away from light. After PI staining solution was added, the percentage of cell apoptosis rate was determined by FACSCalibur.

In terms of cell cycle detection, we fixed the cell suspension with cold ethanol (70%) at 4°C for at least 1 h and then removed ethanol. Following centrifugation and re-rinse of PBS, cells were stained using PI solution (40×, 2 mg/mL: 100 × RNase, 10 mg/mL: 1 × PBS = 25:10:1000) for 30 min. Lastly, FACSCalibur (BD Biosciences) was employed to detect cell cycle distribution (G1, S and G2).

2.7. Wound-healing assay

Glioma SHG-44 and U251 cells were seeded into 6-well dishes. After cell growing for 72 h, we scratched a wound across the cell layer using a 96-wounding replicator (Cat. #VP408FH, VP scientific) and then rinsed slightly for 2–3 times. SHG-44 cells and U251 cells were cultured for 48 h, following which we took fluorescence micrographs and accordingly calculated the cell migration rate.

2.8. Transwell assay

× 10^5 glioma SHG-44 and U251 cells were added to the transwell inner chamber (Cat. # 3422, corning). A total of 600 μL medium containing 30% FBS was added to the external chamber. The inner chamber was placed in the external chamber. Glioma cells were cultured for 24 h. The cells were stained with Giemsa for 5 min. The results were observed and photographed under the microscope, and the cell migration rate was calculated.

2.9. Apoptosis pathway assay

Apoptosis-related proteins and signaling pathways involved in this research were determined utilizing the Human Apoptosis Antibody Array (Cat. #ab134001, Abcam). Simply, after U251 cell samples were washed and lysed, we measured the concentration of the whole proteins via BCA protein assay kit (HyClone-Pierce). The proteins were thus incubated with blocked antibody array membrane throughout the night at 4°C, followed by continue incubation with Streptavidin-HRP for 1 h. Subsequently, we employed enhanced chemiluminescence (ECL) (Amersham) for visualizing proteins and got the gray results by ImageJ software.

2.10. *In vivo* tumorigenesis

Mice used for constructing xenograft models were 28-day-old and BALB/c nude females (Beijing Vitalriver Experimental Animal Technology Co., Ltd), which were randomly separated (shANTXR1 *vs.* shCtrl groups, shANTXR1+AKT activator *vs.* shANTXR1). Nude mice grow in plastic cages without specific pathogens in the SPF animal laboratory of Jiangxi Provincial People's Hospital. They were given 10 h of light every day and could eat and drink freely. Nude mice were subcutaneously injected with 0.2 mL (2×10^7 cells/mL) lentivirus-transfected U251 cell suspensions. The body weight, as well as tumor length and width (for tumor volume) of each mouse model, was first measured after 9 days of the construction of xenograft models, since which the measurement was executed every 6 days for another 4 weeks. In the end, we executed all mice and removed the solid tumors for Ki-67 staining (primary antibody: Ki-67, 1:200, Cat. #ab16667; secondary antibody: HRP, 1:400, Cat. #ab6721, Abcam). Besides, the solid tumors were used for western blotting and

the expression of ANTXR1 (1:2000, Cat. #ab21270, Abcam), p-AKT (1:1000, Cat. #AF887-sp, R&D) and Bcl-2 (1:3000, Cat. #12789–1-AP, Proteintech) was detected. Animal experiments in this research were carried out on a protocol approved by Ethics committee of Jiangxi Provincial People's Hospital, and double-blind experiment was adopted.

2.11. Statistical analysis

We performed cell experiments in triplicate and expressed the data as mean ± SD. Differences between two groups were examined by *t*-test and Mann-Whitney *U* test, with sign test used for the difference in expression patterns of ANTXR1. Spearman correlation test was exploited to estimate the relationship between ANTXR1 level and clinical characteristics, while Kaplan–Meier survival analysis was detecting how high/low level of ANTXR1 affected overall survival of glioma patients. We run all analysis and plotting in SPSS 20.0 and GraphPad Prism software 7.0 with $P < 0.05$ as statistically significant.

3. Results

3.1. Overexpression of *ANTXR1* gene in glioma tissues

The expression patterns of ANTXR1 in glioma tissues and normal brain tissues were detected through immunohistochemical staining. Sign test was subsequently employed to examine the difference in expression patterns of ANTXR1 between glioma tissues and normal brain tissues. The results showed that ANTXR1 was upregulated in glioma tissues in comparison with that in normal tissues ($P < 0.001$) (Figures 1(a-c), Table 1). In regard to clinicopathologic characteristics of the patients with glioma, we also found a significantly positive correlation between the malignant grade of glioma and the expression level of ANTXR1 ($P < 0.01$) (Figure 1d, Tables 2–3). ANTXR1 expression was also more likely to upregulate in the recurrent glioma tissues than in the non-recurrent ones ($P < 0.001$) (Tables 2–3). However, we failed to determine an age- or sex-specific difference in the expression levels of ANTXR1 in patients with glioma ($P > 0.181$) (Table 2). We next utilized Kaplan–Meier survival analysis and found that a higher expression of ANTXR1 predicated a lower survival probability of the glioma patients ($P < 0.05$) (Figure 1b). In view of ANTXR1 overexpression in glioma clinical samples, we next constructed *ANTXR1*-knockdown cell models to examine its potential influences on tumor cell growth and migration.

3.2. Establishment of *ANTXR1*-knockdown model *in vitro*

To build *ANTXR1*-knockdown model in glioma cell lines, we first packaged shRNA targeting *ANTXR1* in lentivirus vector which was labeled by green fluorescent protein (GFP) and established *ANTXR1*-silenced lentivirus. Then, we transfected *ANTXR1*-shRNAs (shANTXR1) or shCtrl lentivirus into SHG-44 and U251 cell lines. After 72 h lentiviral transfection, the inhibitory effects of lentiviral transfection on the *ANTXR1* mRNA level were detected by means of qRT-PCR. The knockdown efficiency of shANTXR1–1 and shANTXR1–2 in SHG-44 cells was 45.6% ($P < 0.01$) and 44.7% ($P < 0.01$), respectively. The knockdown efficiency of shANTXR1–1 and shANTXR1–2 in U251 cells was 55.5% ($P < 0.01$) and 56.1% ($P < 0.01$), respectively (Figure 2a). The following western blotting verified this finding and demonstrated that ANTXR1 protein was notably downregulated in both glioma cell lines in comparison with controls (Figure 2b). Collectively, the *ANTXR1*-knockdown models were successfully established and thus prepared for the following experiments.

3.3. Silencing of *ANTXR1* hampered *in vitro* growth and migration of glioma cells

We next monitored and compared the capacity of cell growth and migration between *ANTXR1*-silenced groups and controls in two cell lines. CCK8 assay unraveled that both cell lines exhibited significantly slower cell proliferation rate in the first 5 consecutive days (SHG-44 cells, $P < 0.001$; U251 cells, $P < 0.001$) in comparison with those in shCtrl group (Figure 3a), indicating a remarkable restriction in cell growth resulted by *ANTXR1* knockdown. Thus, we applied flow

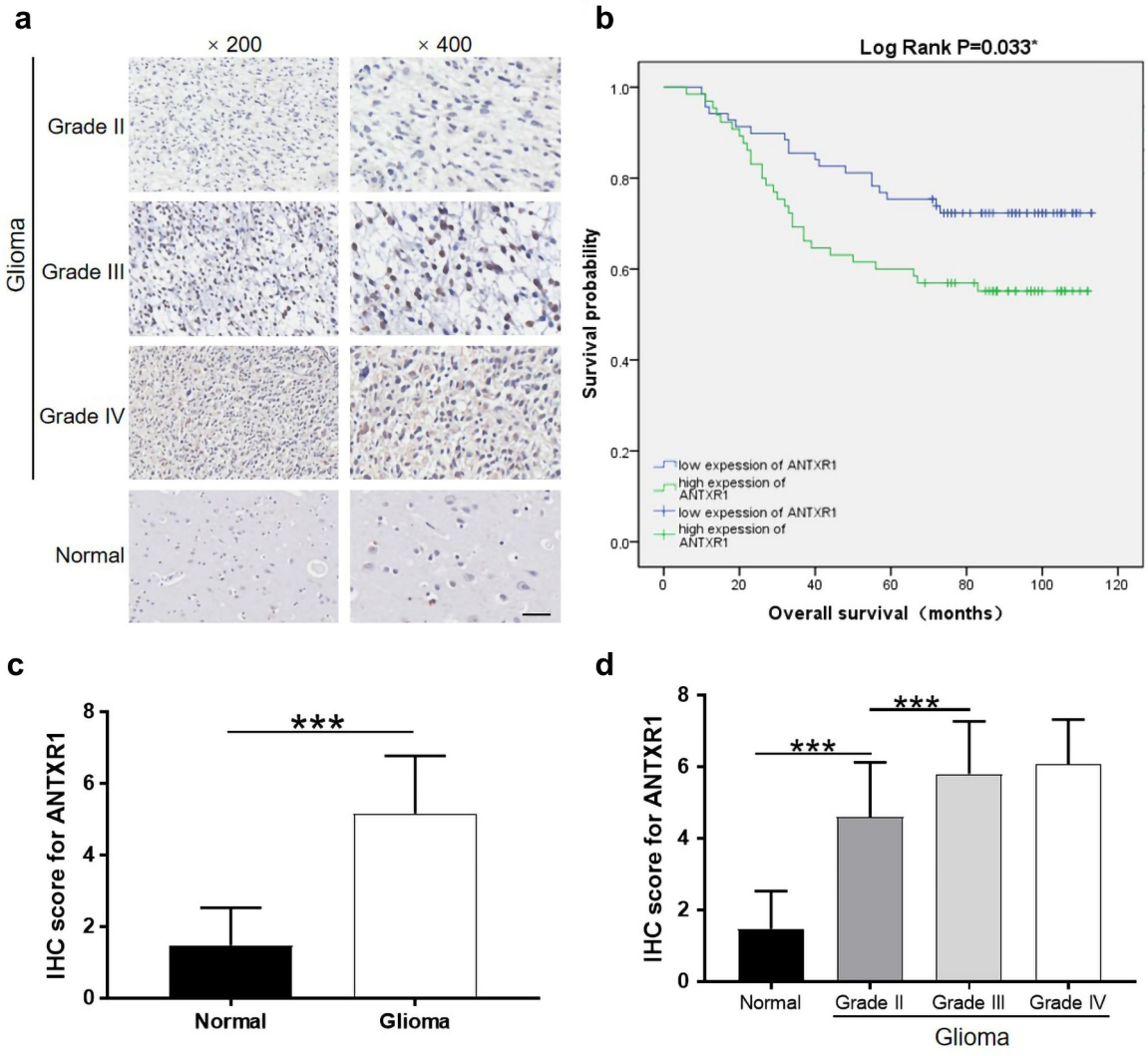

Figure 1. Overexpression of ANTXR1 is related with poor prognosis in glioma. (a) Representative photomicrographs at × 200 and × 400 magnifications of ANTXR1 expression in glioma tissues (grade II-IV) and adjacent normal tissue by immunohistochemical staining. (b) Kaplan–Meier curves of overall survival was used to evaluate the correlation between ANTXR1 expression and prognosis in glioma patients. Significance was obtained using the log rank test. (c) The scores of immunohistochemical staining for ANTXR1 in glioma tissues. (d) The immunohistochemical staining scores of ANTXR1 in glioma tissues of different grades. Scale bar represented 50 μm. ANTXR1, anthrax toxin receptor 1; IHC, immunohistochemical staining. *$P < 0.05$, ***$P < 0.001$.

Table 1. The difference in expression patterns of ANTXR1 between glioma tissues and normal brain tissues suggested by immunohistochemistry. The median IHC staining score was used as the cutoff value.

	Glioma tissue		Normal tissue		
ANTXR1 expression pattern	Cases	Percentage	Cases	Percentage	*P* value
Low	69	51.5%	23	100%	<0.001
High	65	48.5%	0	-	

cytometry to detect cell apoptosis and cell cycle in SHG-44 and U251 cell lines. The results proposed that cell apoptosis was significantly enhanced in shANTXR1–1 and shANTXR1–2 groups (SHG-44 cells, $P < 0.001$; U251 cells, $P < 0.001$) compared with controls (Figure 3b). With regard to cell cycle, we disclosed that knockdown of *ANTXR1* significantly decreased the percentage of cells in G1 phrase in SHG-44 cell line ($P < 0.01$) and U251 cell line ($P < 0.001$) through flow cytometry. Besides, silencing *ANTXR1* significantly reduced the proportion of cells in S phrase (SHG-44 cells,

Table 2. Differences in the expression pattern of ANTXR1 in patients with different glioma/individual features.

Features	No. of patients	ANTXR1 expression pattern		*P* value
		Low	High	
All patients	134	69	65	
Age (years)				0.934
≤43	66	34	32	
>43	67	35	32	
Gender				0.181
Male	88	49	39	
Female	46	20	26	
Tumor recurrence				<0.001
No	52	39	13	
Yes	82	30	52	
Grade				<0.01
II	72	46	26	
III	48	17	31	
IV	14	6	8	

The cutoff age point (43 years old) was the median age of the patients whose ages ranged from 15–80 years old.

Table 3. Results of Spearman correlation analysis between ANTXR1 expression and two tumor characteristics in patients with glioma.

Tumor characteristics	N	Correlation coefficient	*P* value
Grade	134	0.248	<0.01
Tumor recurrence	134	0.375	<0.001

$P < 0.01$; U251 cells, $P < 0.05$) but increased these in G2 phrase in shANTXR1 groups of both cell lines ($P < 0.001$) (Figure 3c), which denoted that ANTXR1 held back cell cycle via targeting G2 phrase during mitosis.

The ability of tumor cell migration was then detected and quantified in both cell lines. The results of wound-healing assay displayed that the cell migration rate (48 h) was markedly lessened ($P < 0.001$ or $P < 0.05$) after harboring shANTXR1 in SHG-44 cells, while it also dropped by the same count in shANTXR1 groups (48 h) compared with controls in U251 cells ($P < 0.01$ or $P < 0.05$) (Figure 4a). The following Transwell assay indicated similar outcomes that knocking down *ANTXR1* was

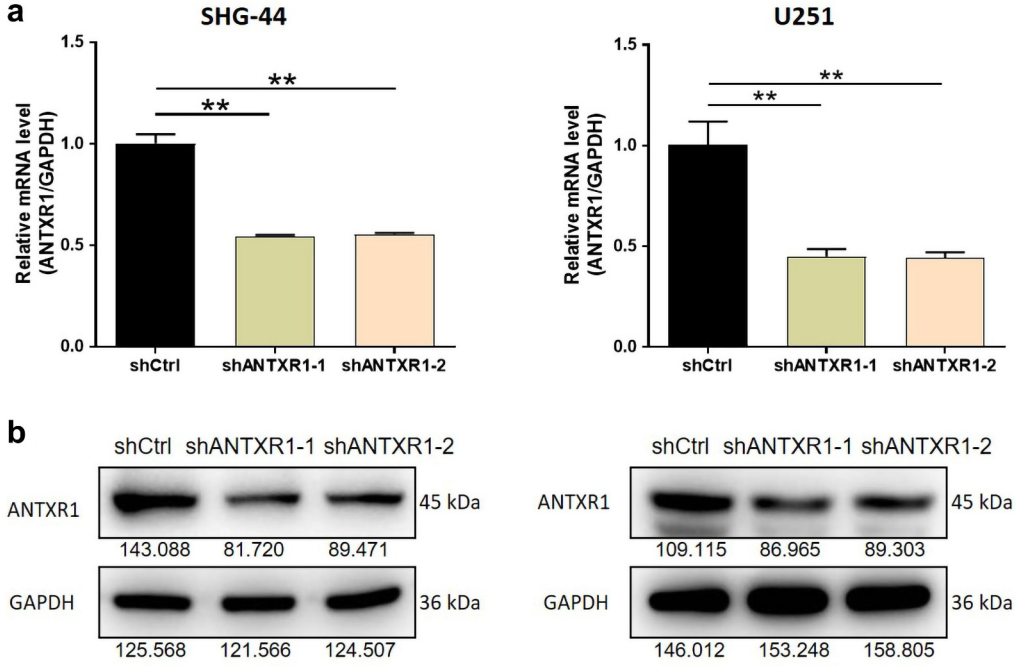

Figure 2. ANTXR1 expression is reduced in glioma cell lines after lentiviral transfection. (A-B) the expression level of *ANTXR1* mRNA and ANTXR1 protein in SHG-44 and U251 cell lines by qRT-PCR and western blotting, respectively. ANTXR1, anthrax toxin receptor 1; shANTXR1, cells transfected by *ANTXR1*-targeting shRNA; shCtrl, cells transfected by control shRNA; GAPDH, glyceraldehyde-3-phosphate dehydrogenase. ($n \geq 3$). ***$P < 0.001$.

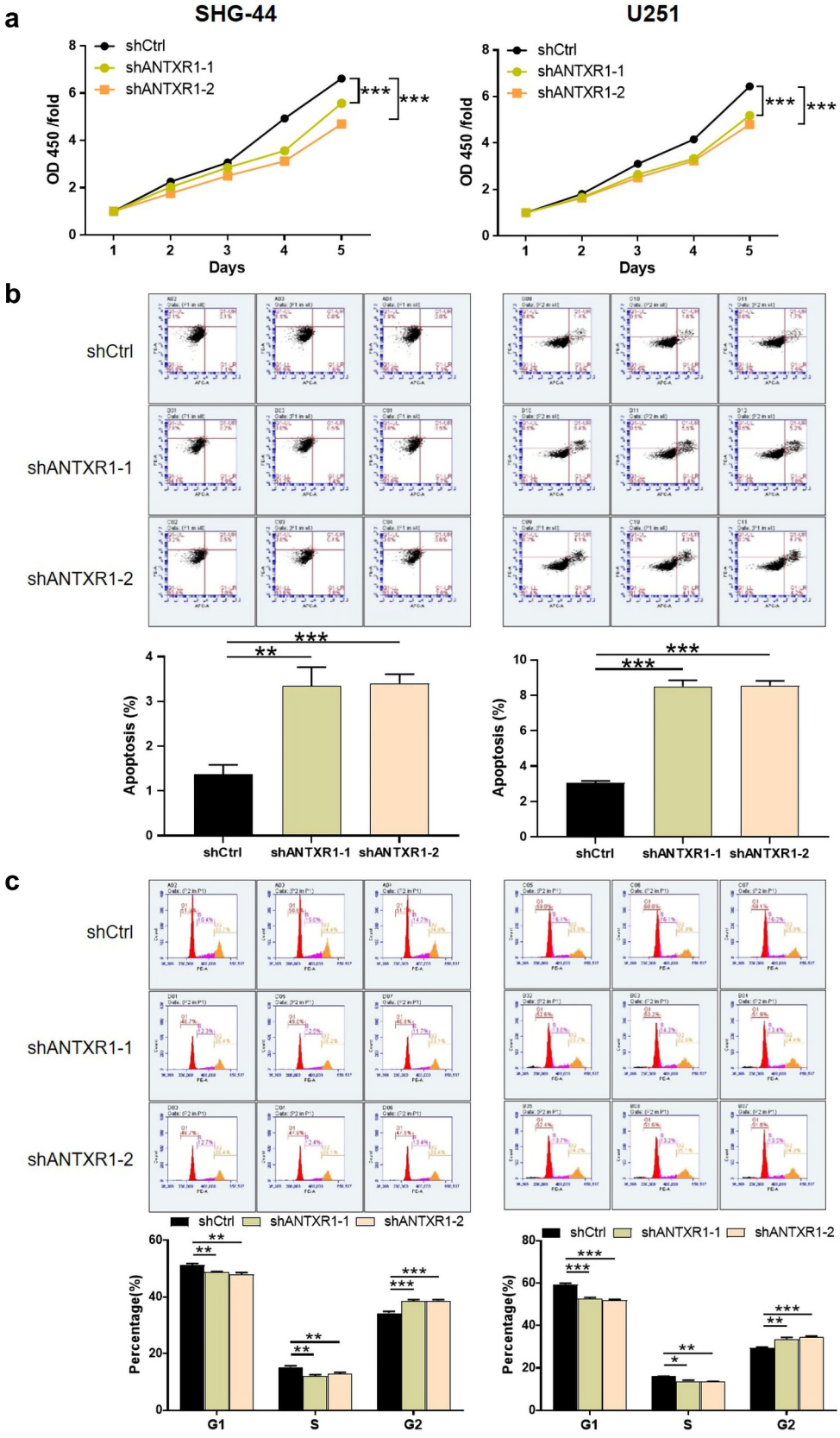

Figure 3. Growth suppression of glioma cells after the transfection of shANTXR1 lentivirus. (a) The effects of shANTXR1 lentivirus (#1 or #2) on the proliferation ability in SHG-44 and U251 cell lines were assessed through CCK8 assay. (b) Cells were stained and the rate of cell apoptosis in two cell lines was obtained through flow cytometry. (c) The distribution of cell cycle in three phrases estimated by flow cytometry. ANTXR1, anthrax toxin receptor 1; shANTXR1, cells transfected by *ANTXR1*-targeting shRNA; shCtrl, cells transfected by control shRNA. $^{**}P < 0.01$, $^{***}P < 0.001$.

associated with 62.7% (shANTXR1–1, $P < 0.001$) and 43% (shANTXR1–2, $P < 0.001$) reduction of migration ability in SHG-44 cells, and 56% (shANTXR1–1, $P < 0.01$) and 49.5% (shANTXR1–2, $P < 0.01$) reduction of migration ability in U251 cells, respectively (Figure 4b). On the whole, our data pointed out ANTXR1 down-expression substantially suppressed glioma cell growth and migration in experimental cell lines *in vitro*.

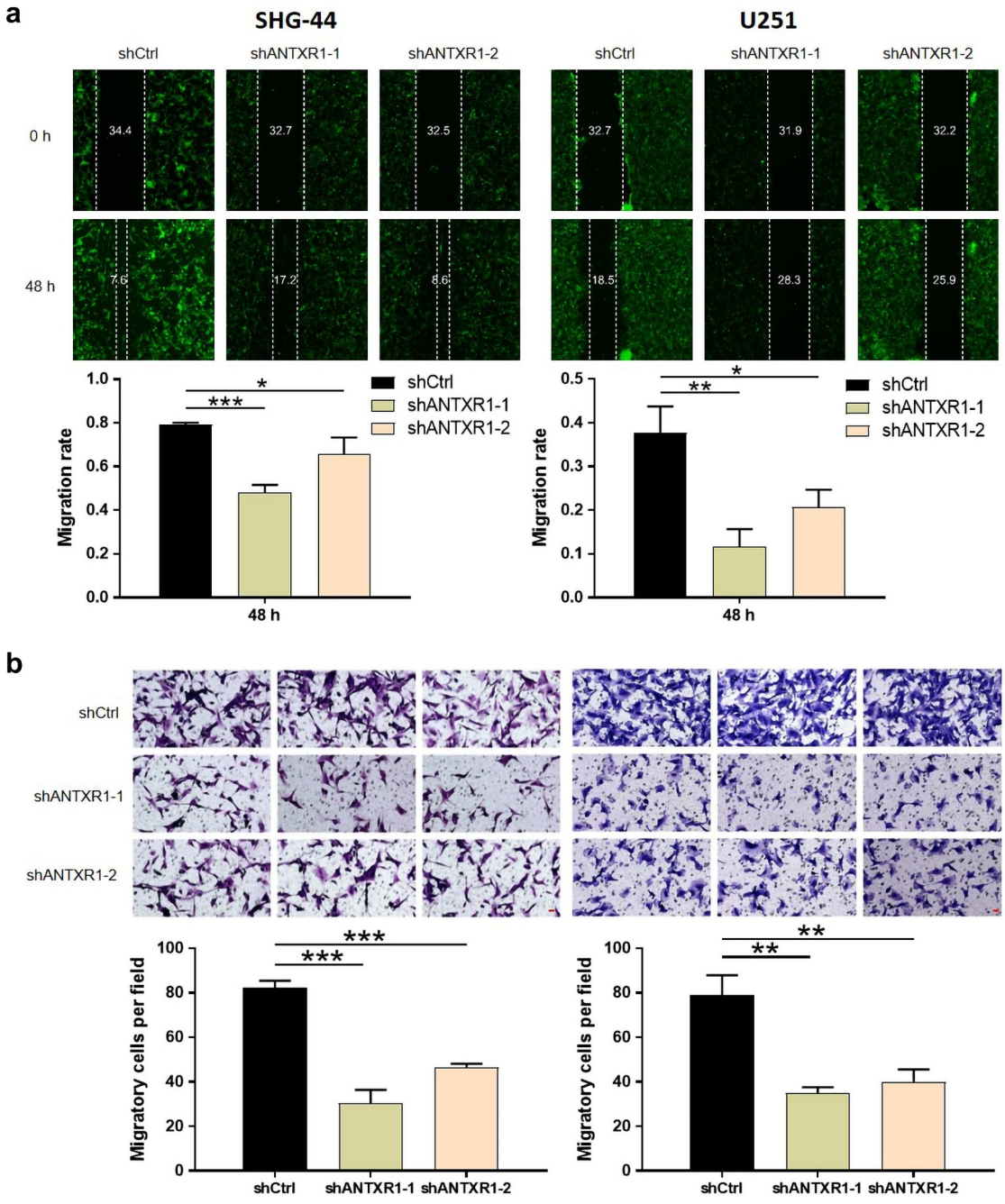

Figure 4. Migration inhibition in shANTXR1-harboring glioma cells. (a) Microphotographs obtained from wound-healing assay and comparison of cell migration between shANTXR1-harboring cells and controls in both cell lines. (b) Representative photographs (×200) of tumor cells after Transwell assay and the comparative results of cell migration between the experimental shANTXR1 group and shCtrl group in SHG-44 and U251 cell lines. ANTXR1, anthrax toxin receptor 1; shANTXR1, cells transfected by *ANTXR1*-targeting shRNA; shCtrl, cells transfected by control shRNA. ***$P < 0.001$.

3.4. Underlying molecular mechanism of ANTXR1 modulating apoptosis in glioma cells

The increment of cell apoptosis rate allowed us for a further human apoptosis antibody array. We perceived that among the human apoptosis-related proteins, HTRA was upregulated with other proteins downregulated (i.e. Bcl-2, Bcl-w, clAP-2, HSP60, HSP70, IGF-I, IGF-II, Livin, sTNF-R2, TNF-α, TNF-β, TRAILR-3, TRAILR-4 and XIAP) after knockdown of *ANTXR1* in the U251 cell line (Figure 5a-c). Western blotting was thereafter employed in U251 tumor cells and the outcomes exhibited an involvement of the upstream MAPK9 signaling pathway. Specifically, the transfection of shANTXR1 had a bearing on the overexpression of MAPK9 but downregulation of P-AKT, CCND1 and CDK6, while the expression level of AKT barely changed in the U251 cell line (Figure 5d).

3.5. ANTXR1 regulated glioma progression via PI3K/AKT pathway

In order to further verify the downstream mechanism of ANTXR1 in glioma cells, we subsequently

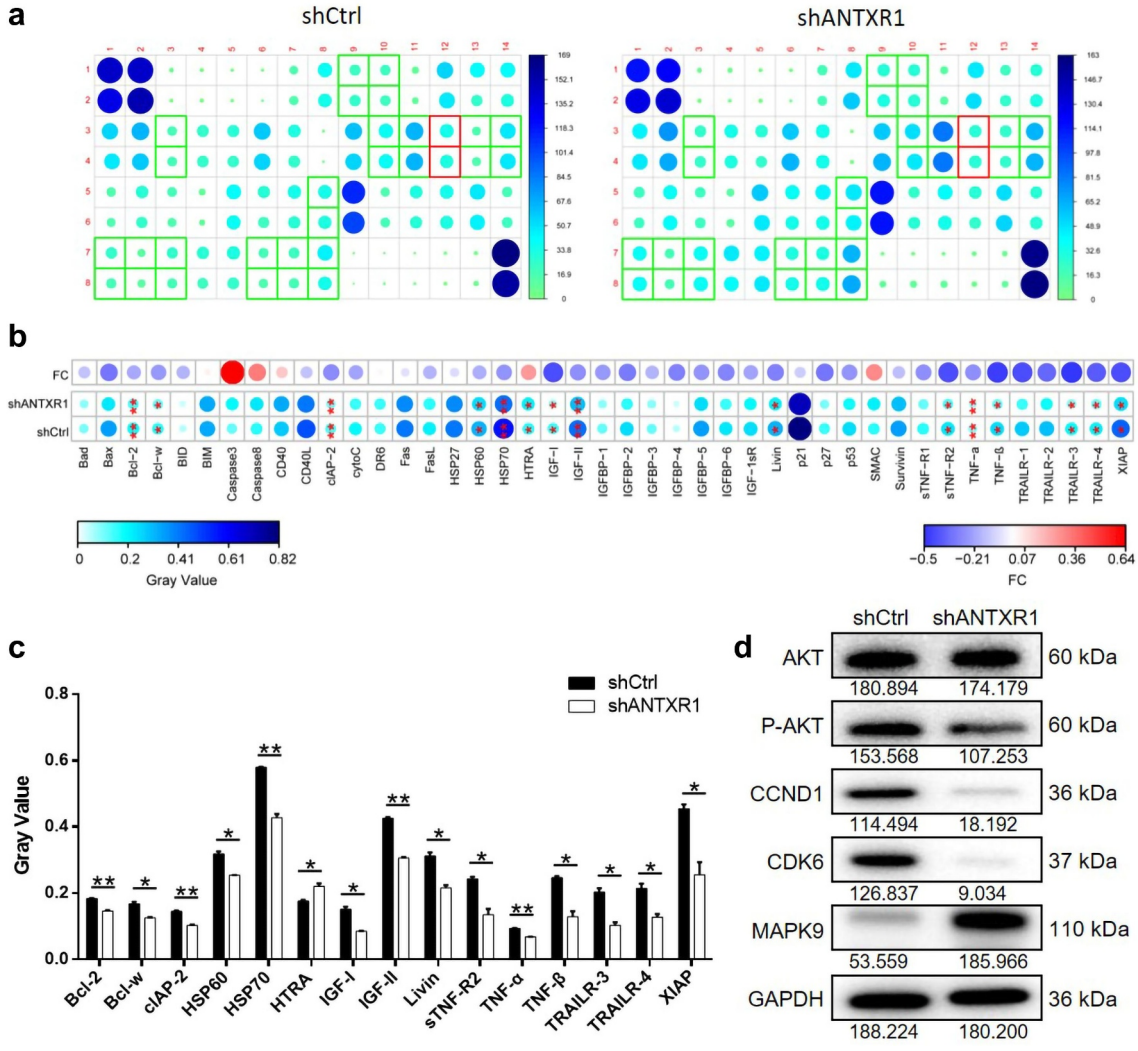

Figure 5. Molecular mechanisms underlying ANTXR1 action in glioma cells. (a-b) the expression level of apoptosis-related proteins in U251 cells treated with shCtrl or shANTXR1 through human apoptosis antibody array. The red box labeled the antibody spots where the signal was significantly reinforced and the green boxes referred to the markedly reduced signals following the transfection of shANTXR1. (c) Comparisons in gray values of 15 apoptosis-related protein markers that were significantly dysregulated in the U251 tumor cells. (d) A western blotting-based detection in the expression of proteins involved in MAPK9 signaling pathway in U251 cells. ANTXR1, anthrax toxin receptor 1; shANTXR1, cells transfected by *ANTXR1*-targeting shRNA; shCtrl, cells transfected by control shRNA. GAPDH, glyceraldehyde-3-phosphate dehydrogenase. $^{*}P < 0.05$, $^{**}P < 0.01$.

detected co-expressed genes of ANTXR1 on the online website (https://www.coexpedia.org/search.php). As a result, there were 481 co-expressed genes which were indeed enriched in cell growth- and cell metastasis-related pathways such as "PI3K/AKT signaling" and "Focal adhesion", based on a Kyoto Encyclopedia of Genes and Genomes (KEGG) database analysis (Figure 6a). We thus carried out a series of cell experiments on U251 cells treated by AKT activator or PI3K inhibitor to verify the regulation of ANTXR1 on PI3K/AKT pathway. As shown in Figure 6b, the AKT, p-AKT, ANTXR1, PI3K and p-PI3K protein levels were examined using western blotting assay in ANTXR1-knockdown U251 cells after disposed by AKT activator. In addition, the expression of

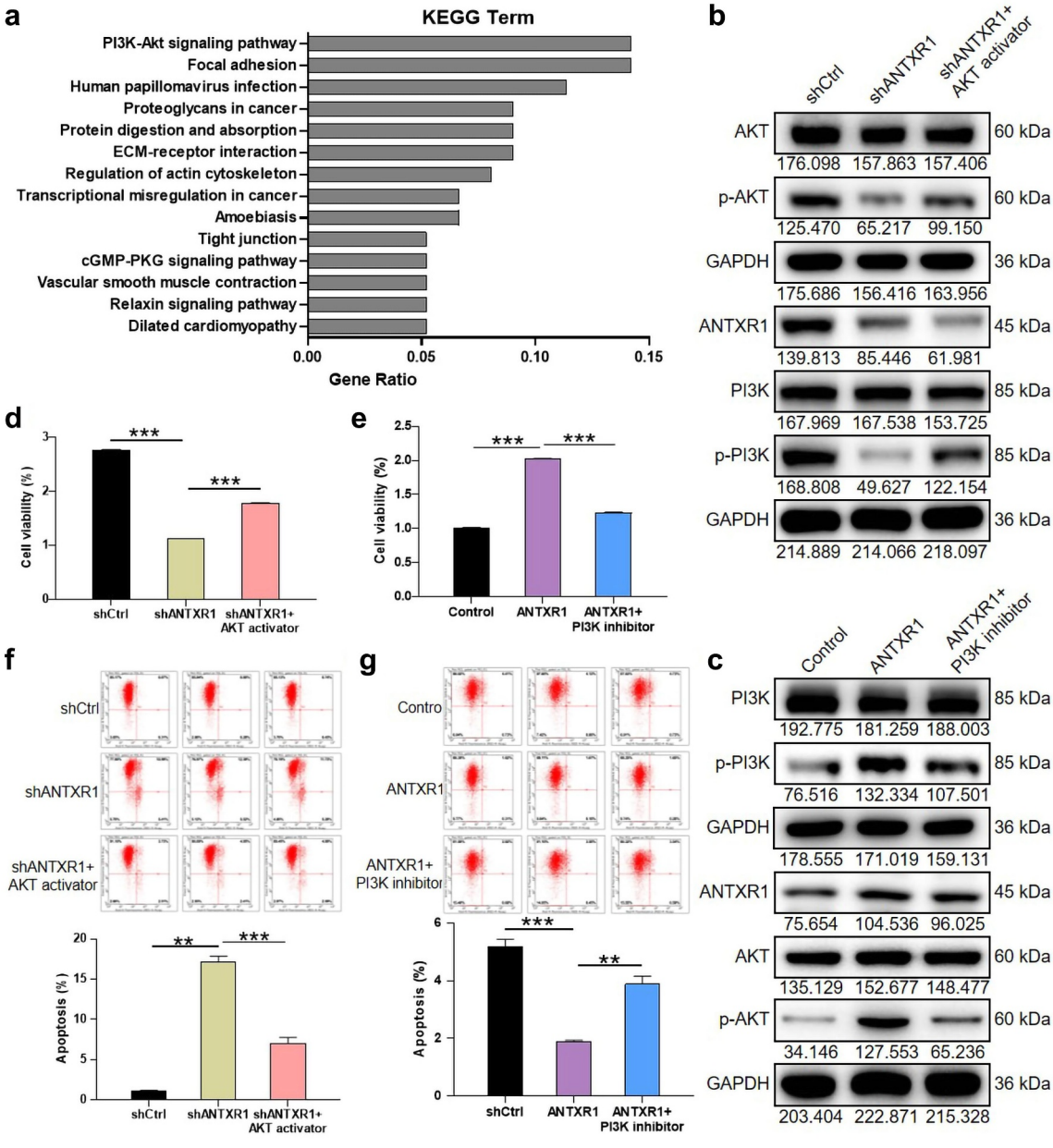

Figure 6. ANTXR1 regulated glioma progression via PI3K/AKT pathway. (a) The top 14 enriched KEGG terms for 481 co-expressed genes of ANTXR1 in human cells. (b) The changes of AKT, p-AKT, ANTXR1, PI3K and p-PI3K expression levels in ANTXR1-knockdown U251 cells after processed by AKT activator. (c) The differences in PI3K, p-PI3K, ANTXR1, AKT and p-AKT levels in ANTXR1-overexpression U251 cells following the treatment of PI3K inhibitor. (d) The influence of AKT activator on cellular viability of shANTXR1-harboring U251 cells, detected by CCK8 assay. (e) Effects of PI3K inhibitor on cellular viability of ANTXR1-overexpression U251 cells, suggested by CCK8 assay. (f) The influence of AKT activator on cell apoptosis of ANTXR1-knockdown U251 cells, examined by FACS. (g) Effects of PI3K inhibitor on cell apoptosis of ANTXR1-overexpression U251 cells, suggested by FACS. $^{**}P < 0.01$, $^{***}P < 0.001$.

PI3K, p-PI3K, ANTXR1, AKT and p-AKT in ANTXR1-overexpression U251 cells following the treatment of PI3K inhibitor was also suggested by western blotting in Figure 6c. Moreover, the results of CCK8 assay indicated that AKT activator could partially recover cellular viability of ANTXR1-knockdown U251 cells resulted by shANTXR1 transfection ($P < 0.001$) (Figure 6d), while PI3K inhibitor imposed significant restriction on the promoted cell viability mediated by the upregulated ANTXR1 ($P < 0.001$) (Figure 6e). Next, as suggested by FACS in Figure 6f, the proportion of apoptotic shANTXR1-harboring U251 cells significantly declined after processed by AKT activator ($P < 0.001$). However, the treatment of PI3K inhibitor considerably promoted cell apoptosis in ANTXR1-overexpression U251 cells ($P < 0.01$) (Figure 6g). In a word, the above-mentioned findings indicated that ANTXR1 participated in cellular malignancy of glioma U251 cells via PI3K/AKT signaling pathway.

3.6. Depletion of ANTXR1 refrained glioma progression *in vivo* via PI3K/AKT pathway

To verify the effect ANTXR1 exerted on glioma progression *in vivo*, we subcutaneously injected SHG-44 cells that were transfected with shCtrl or shANTXR1 (treated/untreated with AKT activator) into nude mice to construct xenograft models and monitored the development of potential tumors. Strikingly, tumor weight of controls also outweighed that after treatment with shANTXR1 lentivirus ($P < 0.01$), whereas after treatment with AKT activator, the tumor weight was remarkably higher than that of ANTXR1 knockdown group ($P < 0.05$) (Figure 7a). The tumor in mice models of the negative controls grew much faster and the volumes were much larger than those in the shANTXR1 group ($P < 0.05$) (Figure 7b). When treated with AKT activator after ANTXR1 knockdown, the tumor volume was larger, and tumor growth was faster than in the ANTXR1 knockdown group ($P < 0.05$) (Figure 7b). Ki-67 staining proved that this proliferation protein marker was notably downexpressed followed by the depletion of ANTXR1 in comparison with that in control group ($P < 0.01$) (Figure 7c-d). Furthermore, western blotting showed that AKT activator partially restored the phosphorylation level of AKT and the level of Bcl-2 protein caused by ANTXR1 knockdown (Figure 7e). As a consequence, disruption of ANTXR1 evoked considerable suppression on *in vivo* tumorigenesis of glioma through PI3K/AKT pathway.

4. Discussion

Unlike other cancers locating noncerebral tissues, glioma is derived from lesions in the primary central nervous system and is seriously threatening mental health. Patients with glioma were also more likely to be cognitively impaired and suffer from more psychological symptoms [17], highlighting the urgent need for more effective treatments of this intractable disorder. This research displayed that in human clinical glioma tissues, ANTXR1 expression was correlated with the severity of the disorder indicated by the clinicopathologic features. Followed by shANTXR1-lentivirus treatment in glioma cell lines, cell apoptosis was substantially promoted *in vitro*, while cell growth and proliferation were limited with similar circumstances encountered in the ability of cell movement and migration. Further western blotting on the regulatory signaling and the downstream apoptosis pathway unveiled the involvement of PI3K/AKT signaling pathway and the alterations of apoptosis-related proteins owing to the silence of *ANTXR1*. Specifically, AKT activator could promote anti-tumor effects mediated by ANTXR1 absence, while PI3K inhibitor confined pro-tumor effects led by upregulated ANTXR1. *In vivo* trials verified the aforementioned findings that the inhibitory effects of *ANTXR1* knockdown were shown on glioma development. In light of these discoveries, we proposed inhibitions on tumor growth driven by *ANTXR1* knockdown with the involvement of PI3K/AK pathway in glioma patients.

Consistently, it has been reported that ANTXR1 was upregulated and *miR-26b-3p* acted as its critical upstream modulator in glioma progression [15]. The present study tried to unfold and trace its downstream regulatory mechanisms. The findings here implied the pivotal role of ANTXR1 in MAPK signaling pathway as its upstream deactivator since downregulation of MAPK9 was greatly attributable to the presence of ANTXR1. MAPK

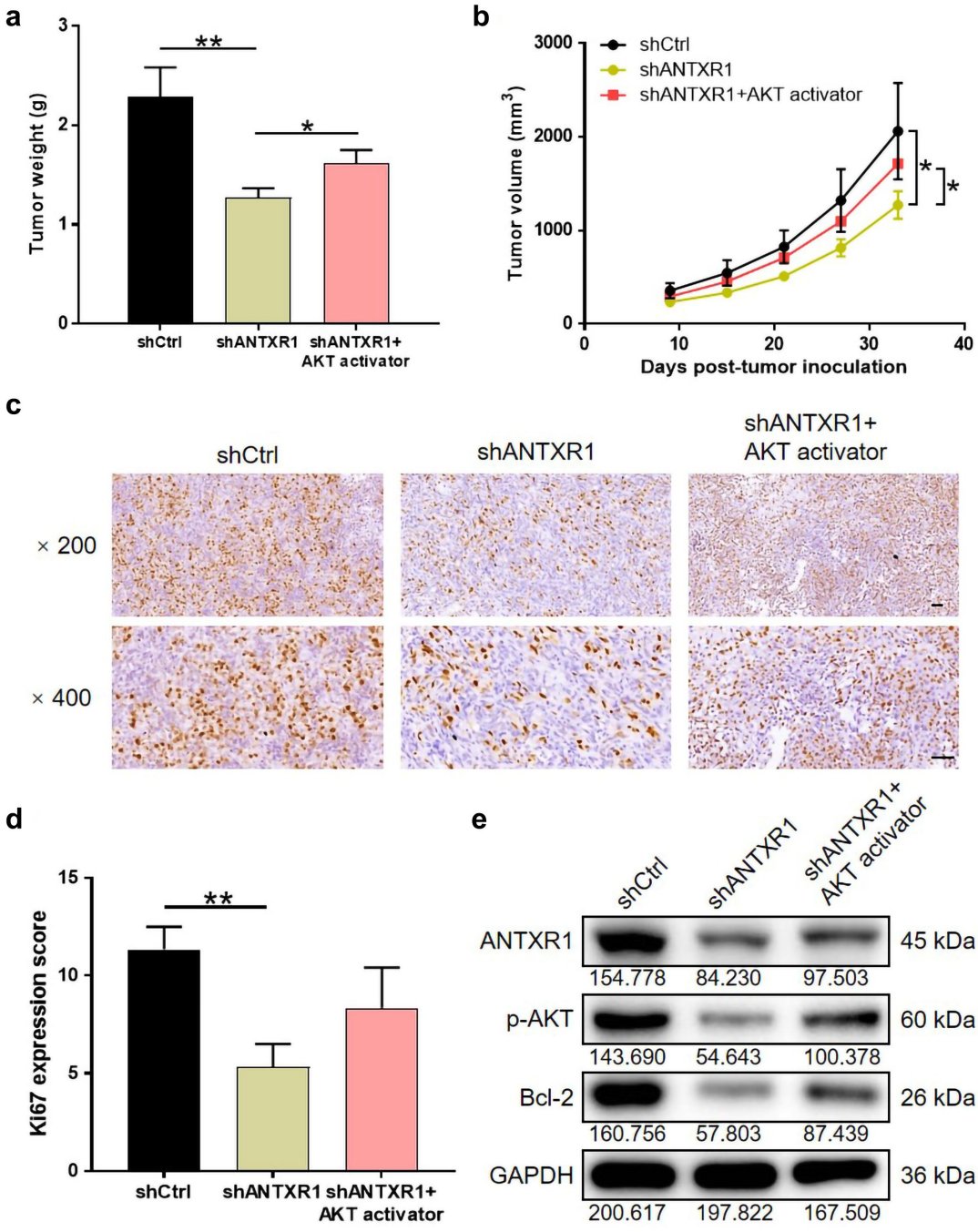

Figure 7. Depleting ANTXR1 *in vivo* alleviated glioma progression via PI3K/AKT pathway. (a) The comparison in weight of solid tumors taken out from mice models. (b) The quantified comparison of xenograft tumor volumes (shCtrl *vs*. shANTXR1, shANTXR1 *vs*. shANTXR1+AKT activator, $n = 3$ each group). (c) Microphotographs of cells after Ki-67 staining assay in shCtrl, shANTXR1 and shANTXR1+AKT activator groups of U251 cells (×200 and × 400, respectively). Scale bar represented 50 μm. (d) The scores of Ki67 immunohistochemical staining. (e) The expression levels of ANTXR1, p-AKT and Bcl-2 in shCtrl, shANTXR1 and shANTXR1+AKT activator groups were detected by western blotting. ANTXR1, anthrax toxin receptor 1; shANTXR1, cells transfected by *ANTXR1*-targeting shRNA; shCtrl, cells transfected by control shRNA. *$P < 0.05$, **$P < 0.01$.

(mitogen-activated protein kinase) signaling cascades include several signaling components (RAS-MAPK) and have been suggested to participate in mediating cellular signal transmissions, thus regulating cell growth and proliferation [18]. This pathway is involved in numerous biological processes, and its dysregulation was commonly found in many syndromes and disorders, including

a number of human tumors. MAPK9, also known as JNK2, is a member of MAPKs targeting specific transcription factors and thus modulates gene expression during the cell-cycle process [19]. In colitis-induced colorectal carcinoma, MAPK9 functioned as a tumor suppressor and inflammation-triggered inactivation of MAPK9 would result in abnormalities of MAPK9-dependent cell cycle [20]. MAPK9 deficiency was also found to support the development of breast cancer [21]. Nevertheless, the carcinostasis of MAPK9 was not always true. In melanoma, MAPK9 played a positive role in cell proliferation and its activity was of the essence in tumorigenesis [22].

Additionally, ANTXR1 shortage also led to reduction of AKT phosphorylation. The AKT activator promoted viability and inhibited apoptosis of shANTXR1-harboring glioma cells, while PI3K inhibitor confined viability and facilitate apoptosis of ANTXR1-overexpression glioma cells. These findings implied that silencing *ANTXR1* blocked tumorigenesis through inactivating PI3K/AKT signaling pathway and further dysregulating CDKs. In our experiments, CDK6, which was particularly needed for G1/S transition, were found downregulated in glioma cell lines following depletion of ANTXR1. This result proposed an ANTXR1-mediated association between MAPK9 inactivation and the expression of cell cycle-related proteins. CCND1, also named cyclin D1, functioned as a regulatory subunit of CDK4 or CDK6, both of which were vital regulators in the stepwise progression of cell cycle [23]. CCND1 was considered to be a pan-cancer actor, and dysregulation of CCND1 had linkage with pathogenesis of human tumors, e.g. prostate cancer, retinoblastoma [24] and head and neck squamous cell carcinoma [25]. Amplification of *CCND1* also conferred unfavorable prognosis in malignant tumors [26]. In agreement with this, we also demonstrated an ANTXR1-mediated cell cycle disruption and growth promotion via activating PI3K/AKT signaling pathway in glioma patients.

Regarding the downstream apoptosis pathway, we declared a series of decreases in apoptosis-related proteins but an increase in HTRA2 following depletion of ANTXR1. HTRA2 (high-temperature requirement A2), locating in the mitochondrial inter membrane, has been reported to bind apoptosis inhibitory factors and evoke cell apoptosis to maintain mitochondrial homeostasis, which acknowledgedly serves as a favorable target for anticancer agents [27]. In prostate cancer, a reduction in HTRA2 abrogated cell apoptotic activity through interacting with C-terminus of ITGA7, a primary laminin receptor [28]. Intracerebral hemorrhage in rat models gave rise to upregulation of HTRA2 and initiated HTRA2-triggered neuronal apoptosis [29]. Researchers previously announced that HTRA2 performed its pro-apoptotic function by interacting with XIAP (X-linked inhibitor of apoptosis protein) in a caspase-dependent manner [30]. Consistent with this notion, after silencing *ANTXR1*, our study also detected downexpression of XIAP but overexpression of HTRA2. We hence drew the conclusion that ANTXR1-mediated dysregulation of PI3K/AKT pathway in glioma cells contributed to abnormalities in apoptotic pathway by downregulating HTRA2.

In summary, we investigated the ANTXR1 role and its downstream molecular mechanisms in regulating malignant biological behaviors of glioma. Our results sounded ANTXR1 acted as a tumor promoter in glioma induction via activating PI3K/AKT-mediated cell proliferation. There is still a deficiency in this study, that is, it cannot be determined which apoptosis related protein ANTXR1 regulates glioma cell apoptosis, which will be further explored in future research. In conclusion, findings from this study, in conjunction with previous work on ANTXR1 can provide a promising option as anticancer agents for the clinical therapeutics of glioma.

Disclosure statement

No potential conflict of interest was reported by the author(s).

Funding

The work was supported by the Science and Technology Plan Projects of Health Commission of Jiangxi Province [202310002]; Science and Technology Research Project of Jiangxi Provincial Education Department [GJJ2203526]; Science and Technology Research Project of Jiangxi Provincial Education Department [GJJ2203524]; Science and Technology Plan Projects of Health Commission of Jiangxi Province [202310105].

Authors' contributions

Dengfeng Wan, Aijun Liang and Chaoyang Zhou have made substantial contributions to the concept and design of this study. Jianzhong Zhang, Jingxing Leng, Bin Xi and Bin Zhou, conducted the experiments. Yu Yang, Ronglan Zhu, Liangchen Zhong and Xingxing Jiang conducted data analysis. Aijun Liang and Chaoyang Zhou produced the manuscript. All authors have approved the final draft.

Data availability statement

All data generated and analyzed during this study are included in this published article and its supplementary information files.

Ethical statement

Animal experiments in this research were carried out on a protocol approved by Ethics committee of Jiangxi Provincial People's Hospital.

References

[1] Giese A, Bjerkvig R, Berens ME, et al. Cost of migration: invasion of malignant gliomas and implications for treatment. JCO. 2003 Apr 15;21(8):1624–1636. doi: 10.1200/JCO.2003.05.063

[2] Weller M, Wick W, Aldape K, et al. Glioma. Nature reviews disease primers. Nat Rev Dis Primers. 2015 Jul 16;1(1):15017. doi: 10.1038/nrdp.2015.17

[3] Lavon I, Refael M, Zelikovitch B, et al. Serum DNA can define tumor-specific genetic and epigenetic markers in gliomas of various grades. Neuro Oncol. 2010 Feb;12 (2):173–180. doi: 10.1093/neuonc/nop041

[4] Bai R-Y, Staedtke V, Riggins GJ. Molecular targeting of glioblastoma: drug discovery and therapies. Trends Mol Med. 2011 June 01;17(6):301–312. doi:10.1016/j.molmed.2011.01.011.

[5] Gorovets D, Kannan K, Shen R, et al. IDH mutation and neuroglial developmental features define clinically distinct subclasses of lower grade diffuse astrocytic glioma. Clin Cancer Res. 2012 May 1;18 (9):2490–2501. doi: 10.1158/1078-0432.CCR-11-2977

[6] Wen PY, Reardon DA. Neuro-oncology in 2015: Progress in glioma diagnosis, classification and treatment. Nat Rev Neurol. 2016 Feb;12(2):69–70. doi: 10.1038/nrneurol.2015.242

[7] Jayawardena N, Burga LN, Easingwood RA, et al. Structural basis for anthrax toxin receptor 1 recognition by Seneca Valley Virus. Proc Natl Acad Sci, USA. 2018 Nov 13;115(46):E10934–e10940. doi: 10.1073/pnas.1810664115

[8] Bachran C, Leppla SH. Tumor targeting and drug delivery by anthrax toxin. Toxins (Basel). 2016 Jul 1;8 (7):197. doi:10.3390/toxins8070197

[9] Nanda A, Carson-Walter EB, Seaman S, et al. TEM8 interacts with the cleaved C5 domain of collagen alpha 3(VI). Cancer Res. 2004 Feb 1;64(3):817–820. doi: 10.1158/0008-5472.CAN-03-2408

[10] Bradley KA, Mogridge J, Mourez M, et al. Identification of the cellular receptor for anthrax toxin. Nature. 2001 Nov 8;414(6860):225–229. doi: 10.1038/n35101999

[11] Gutwein LG, Al-Quran SZ, Fernando S, et al. Tumor endothelial marker 8 expression in triple-negative breast cancer. Anticancer Res. 2011 Oct;31(10):3417–3422.

[12] Singh AP, Bafna S, Chaudhary K, et al. Genome-wide expression profiling reveals transcriptomic variation and perturbed gene networks in androgen-dependent and androgen-independent prostate cancer cells. Cancer Lett. 2008 Jan 18;259(1):28–38. doi: 10.1016/j.canlet.2007.09.018

[13] Jinnin M, Medici D, Park L, et al. Suppressed NFAT-dependent VEGFR1 expression and constitutive VEGFR2 signaling in infantile hemangioma. Nature Med. 2008 Nov;14(11):1236–1246. doi: 10.1038/nm.1877

[14] Chaudhary A, Hilton Mary B, Seaman S, et al. TEM8/ANTXR1 blockade inhibits pathological angiogenesis and potentiates tumoricidal responses against multiple cancer types. Cancer Cell. 2012 Feb 14;21(2):212–226. doi: 10.1016/j.ccr.2012.01.004

[15] Geng F, Lu G-F, Ji M-H, et al. MicroRNA-26b-3p/ANTXR1 signaling modulates proliferation, migration, and apoptosis of glioma. Am J Transl Res. 2019;11 (12):7568–7578.

[16] Louis DN, Perry A, Reifenberger G, et al. The 2016 world Health Organization classification of tumors of the central nervous System: a summary. Acta Neuropathol. 2016 Jun;131(6):803–820. doi: 10.1007/s00401-016-1545-1

[17] Giovagnoli AR, Silvani A, Colombo E, et al. Facets and determinants of quality of life in patients with recurrent high grade glioma. J Neurol Neurosurg Psychiatry. 2005 Apr;76(4):562–568. doi: 10.1136/jnnp.2004.036186

[18] McCubrey JA, Steelman LS, Chappell WH, et al. Roles of the Raf/MEK/ERK pathway in cell growth, malignant transformation and drug resistance. Biochim Biophys Acta, Mol Cell Res. 2007 Aug;1773 (8):1263–1284. doi: 10.1016/j.bbamcr.2006.10.001

[19] Waetzig V, Wacker U, Haeusgen W, et al. Concurrent protective and destructive signaling of JNK2 in neuroblastoma cells. Cell Signal. 2009 Jun;21(6):873–880. doi: 10.1016/j.cellsig.2009.01.032

[20] Lessel W, Silver A, Jechorek D, et al. Inactivation of JNK2 as carcinogenic factor in colitis-associated and sporadic colorectal carcinogenesis. Carcinogenesis. 2017 May 1;38(5):559–569. doi: 10.1093/carcin/bgx032

[21] Cellurale C, Girnius N, Jiang F, et al. Role of JNK in mammary gland development and breast cancer. Cancer Res. 2012 Jan 15;72(2):472–481. doi: 10.1158/0008-5472.CAN-11-1628

[22] Du L, Anderson A, Nguyen K, et al. JNK2 is required for the tumorigenic properties of melanoma cells. ACS Chem Biol. 2019 Jul 19;14(7):1426–1435. doi: 10.1021/acschembio.9b00083

[23] Casimiro MC, Velasco-Velázquez M, Aguirre-Alvarado C, et al. Overview of cyclins D1 function in cancer and the CDK inhibitor landscape: past and present. Expert Opin Investig Drugs. 2014 March 01;23(3):295–304. doi: 10.1517/13543784.2014.867017

[24] Mizuarai S, Machida T, Kobayashi T, et al. Expression ratio of CCND1 to CDKN2A mRNA predicts RB1 status of cultured cancer cell lines and clinical tumor samples. Mol Cancer. 2011 Mar 29;10(1):31. doi: 10.1186/1476-4598-10-31

[25] Callender T, el-Naggar AK, Lee MS, et al. PRAD-1 (CCND1)/cyclin D1 oncogene amplification in primary head and neck squamous cell carcinoma. Cancer. 1994 Jul 1;74(1):152–158. doi: 10.1002/1097-0142(19940701)74:1<152:AID-CNCR2820740124>3.0.CO;2-K

[26] Moradi Binabaj M, Bahrami A, Khazaei M, et al. The prognostic value of cyclin D1 expression in the survival of cancer patients: a meta-analysis. Gene. 2020 Feb 20;728:144283. doi:10.1016/j.gene.2019.144283

[27] Zurawa-Janicka D, Skorko-Glonek J, Lipinska B. HtrA proteins as targets in therapy of cancer and other diseases. Expert opinion on therapeutic targets. Expert Opin Ther Targets. 2010 Jul;14(7):665–679. doi: 10.1517/14728222.2010.487867

[28] Zhu Z-H, Yu YP, Zheng Z-L, et al. Integrin alpha 7 interacts with high temperature requirement A2 (HtrA2) to induce prostate cancer cell death. Am J Pathol. 2010 Sep 01;177(3):1176–1186. doi: 10.2353/ajpath.2010.091026

[29] Sun H, Li L, Zhou F, et al. The member of high temperature requirement family HtrA2 participates in neuronal apoptosis after intracerebral hemorrhage in adult rats. J Mol Hist. 2013 Aug;44(4):369–379. doi: 10.1007/s10735-013-9489-4

[30] Liu HR, Gao E, Hu A, et al. Role of Omi/HtrA2 in apoptotic cell death after myocardial ischemia and reperfusion. Circulation. 2005 Jan 4;111(1):90–96. doi: 10.1161/01.CIR.0000151613.90994.17